The Meteoritical Society

Meteoritics & Planetary Science 51, Nr 9, 1643–1653 (2016)
doi: 10.1111/maps.12687

Replacement of glass in the Nakhla meteorite by berthierine: Implications for understanding the origins of aluminum-rich phyllosilicates on Mars

Martin R. LEE[1*] and Elias CHATZITHEODORIDIS[2]

[1]School of Geographical and Earth Sciences, University of Glasgow, Gregory Building, Lilybank Gardens, Glasgow G12 8QQ, UK
[2]Department of Geological Sciences, School of Mining and Metallurgical Engineering, National Technical University of Athens, Athens, Greece
[*]Corresponding author. E-mail: martin.lee@glasgow.ac.uk

(Received 12 February 2016; revision accepted 02 June 2016)

Abstract–A scanning and transmission electron microscope study of aluminosilicate glasses within melt inclusions from the Martian meteorite Nakhla shows that they have been replaced by berthierine, an aluminum-iron serpentine mineral. This alteration reaction was mediated by liquid water that gained access to the glasses along fractures within enclosing augite and olivine grains. Water/rock ratios were low, and the aqueous solutions were circumneutral and reducing. They introduced magnesium and iron that were sourced from the dissolution of olivine, and exported alkalis. Berthierine was identified using X-ray microanalysis and electron diffraction. It is restricted in its occurrence to parts of the melt inclusions that were formerly glass, thus showing that under the ambient physico-chemical conditions, the mobility of aluminum and silicon were low. This discovery of serpentine adds to the suite of postmagmatic hydrous silicates in Nakhla that include saponite and opal-A. Such a variety of secondary silicates indicates that during aqueous alteration compositionally distinct microenvironments developed on sub-millimeter length scales. The scarcity of berthierine in Nakhla is consistent with results from orbital remote sensing of the Martian crust showing very low abundances of aluminum-rich phyllosilicates.

INTRODUCTION

Meteorites from Mars are a unique and powerful source of information on the planet's geological history (e.g., McSween 1985, 1994; Treiman 2005; Velbel 2012). These rocks are of particular current interest owing to the insights that they can provide into the presence, longevity, and properties of liquid water in the Martian crust. The former occurrence of water can be revealed by etch pits in minerals including olivine (Velbel 2012; Lee et al. 2013; Tomkinson et al. 2013; Velbel 2016). Martian water can also be studied directly because it is contained within hydrous and nominally anhydrous primary (i.e., magmatic) components (e.g., apatite, amphibole, olivine, glass), shock-formed glasses, and aqueous alteration products (e.g., phyllosilicates) (Watson et al. 1994; Leshin et al. 1996; Boctor et al. 2003; Usui et al. 2012, 2015; Hallis et al. 2012a, 2012b; Hu et al. 2014). The provenance of this water can be investigated using the deuterium/hydrogen (D/H) system (Watson et al. 1994; Leshin et al. 1996). Results of such work have shown that the magmatic components contain water with either a low D/H mantle signature, or with higher D/H ratios indicating isotopic equilibration with the D-rich Martian atmosphere (Usui et al. 2012, 2015; Hallis et al. 2012b). The products of aqueous alteration have atmospheric D/H values (Leshin et al. 1996; Hallis et al. 2012a).

The identity and diversity of aqueous alteration products in the Martian meteorites can give further insights into the nature of the interaction of groundwater with crustal rocks. These secondary components are most abundant in the nakhlite meteorites where they include hydrous silicates, carbonates, oxides and hydroxides, halides, and sulfates (Ashworth and Hutchison 1975; Bunch and Reid 1975; Gooding et al. 1991; Treiman 1993; Bridges and Grady 2000; Velbel 2012). Here, we have studied silicates,

which are the volumetrically dominant alteration products and so they can be used most effectively to explore the nature and properties of the groundwater system (e.g., length scale, longevity, chemistry). We have focused on the Nakhla meteorite because early work concluded that it has a low diversity of secondary hydrous silicates (Ashworth and Hutchison 1975; Gooding et al. 1991), thus suggesting that the water was compositionally homogeneous. Subsequent research has, however, identified opal-A (Lee et al. 2015a), and a complex saponite-rich structure (Chatzitheodoridis et al. 2014), thus suggesting a more heterogeneous aqueous system. We have built on these recent findings by seeking other alteration products, and our search has concentrated on melt inclusion glasses within olivine phenocrysts. As they are chemically distinct from the ferromagnesian silicate minerals that are the most abundant constituents of Nakhla, we hypothesize that the interaction of these glasses with liquid water moving through their parent rock could produce minerals that have not been previously recorded from this meteorite. Results of our work demonstrate that glass in some of these inclusions has been altered to berthierine, an Al-Fe-serpentine mineral. As it is the first description of this phyllosilicate mineral from Nakhla, these results can provide fresh insights into the nature of water–rock interaction in the Martian crust.

MATERIALS AND METHODS

Nakhla fell near to the village of El Nakhla El Baharia, Egypt, in 1911 (Prior 1912). Two samples of this meteorite were studied, both of which were loaned by the Natural History Museum, London: BM1911,369, p.7963 (a glass-mounted wafer 60 μm in thickness), and BM1913,26, no. 2 (a polished block). They are hereafter referred to as BM1911 and BM1913, respectively.

After being coated with a ~10 nm layer of carbon, these samples were studied using two field-emission SEMs at the University of Glasgow, both operated at 20 kV: a FEI Quanta 200F and a Zeiss Sigma. These microscopes are equipped with silicon-drift energy-dispersive X-ray (EDX) detectors. The Quanta operates through an EDAX Genesis microanalysis system and the Zeiss through an Oxford Instruments Aztec system. Both SEMs were used for qualitative X-ray microanalysis and the acquisition of backscattered electron (BSE) images, whose contrast relates mainly to spatial variations in mean atomic number, Z. Two SEMs were used for quantitative chemical analysis by EDX: the Zeiss Sigma, and a JEOL JSM-6310 at the University of Graz. The Zeiss was operated at 20 kV/2 nA, with the electron beam rastered over an area of ~2 × 2 μm, and spectra were acquired for 60 s. Calibration used the following mineral standards: jadeite (Na), periclase (Mg), corundum (Al), rhodonite (Si, Mn), orthoclase (K), diopside (Ca), rutile (Ti), chromite (Cr), and garnet (Fe). Typical detection limits were as follows (in wt% element): Na (0.04), Mg (0.05), Al (0.06), Si (0.07), K (0.08), Ca, Ti (0.12), Cr, Mn (0.14), Fe (0.18). The JEOL JSM-6310 was operated at 15 kV with a spot size of ~1 μm. Spectra were collected for 100 s, and quantified using an Oxford Instruments system. Internal laboratory standards were used to configure the instrument for quantitative analyses, and standardization was performed on the same day and prior to acquisition of X-ray spectra.

In order to preserve material for later studies, transmission electron microscopy (TEM) work was undertaken only on BM1911. Two foils were cut and extracted from one of its melt inclusions using a FEI Nanolab dual beam focused ion beam (FIB) instrument and following the procedure of Lee et al. (2003). Both foils were 11 × 5 × 0.1 μm in size. Bright-field images, high-resolution images, and selected area electron diffraction (SAED) patterns were acquired from these foils using a FEI T20 TEM operated at 200 kV. Quantitative chemical analyses were obtained by scanning TEM (STEM) using a JEOL ARM200F that was operated at 200 keV/~180 pA. Chemical analyses were acquired in STEM mode and using a Bruker 60 mm^2 SDDEDX spectrometer. The electron beam was rastered over an area of ~100 by 100 nm for a live time of 30 s. EDX spectra were quantified using Bruker software and following a standardless Cliff-Lorimer procedure.

RESULTS

Petrographic Context of the Melt Inclusions

Nakhla is a cumulate olivine clinopyroxenite. It crystallized at ~1.33 Ga (Swindle and Olson 2004) in a shallow lava flow or sill (Friedman-Lentz et al. 1999). Needham et al. (2013) determined that this meteorite has a modal mineralogy of 79.4 vol% pyroxene (mainly augite), 9.5 vol% olivine, and 11.1 vol% mesostasis (the mesostasis is dominated by laths of plagioclase feldspar and titanomagnetite crystals; Treiman 2005). Nakhla also hosts ~1 wt% of aqueous alteration products that occur mainly in olivine grains, and rarely within augite crystals and the mesostasis (Ashworth and Hutchison 1975; Bunch and Reid 1975; Lee et al. 2013, 2015a). These secondary components, which include opal-A and saponite, contain the majority of Nakhla's 0.11–0.13 wt% water (Karlsson et al. 1992; Leshin et al. 1996). The melt inclusions studied here have originated from the trapping of small volumes of magma during the

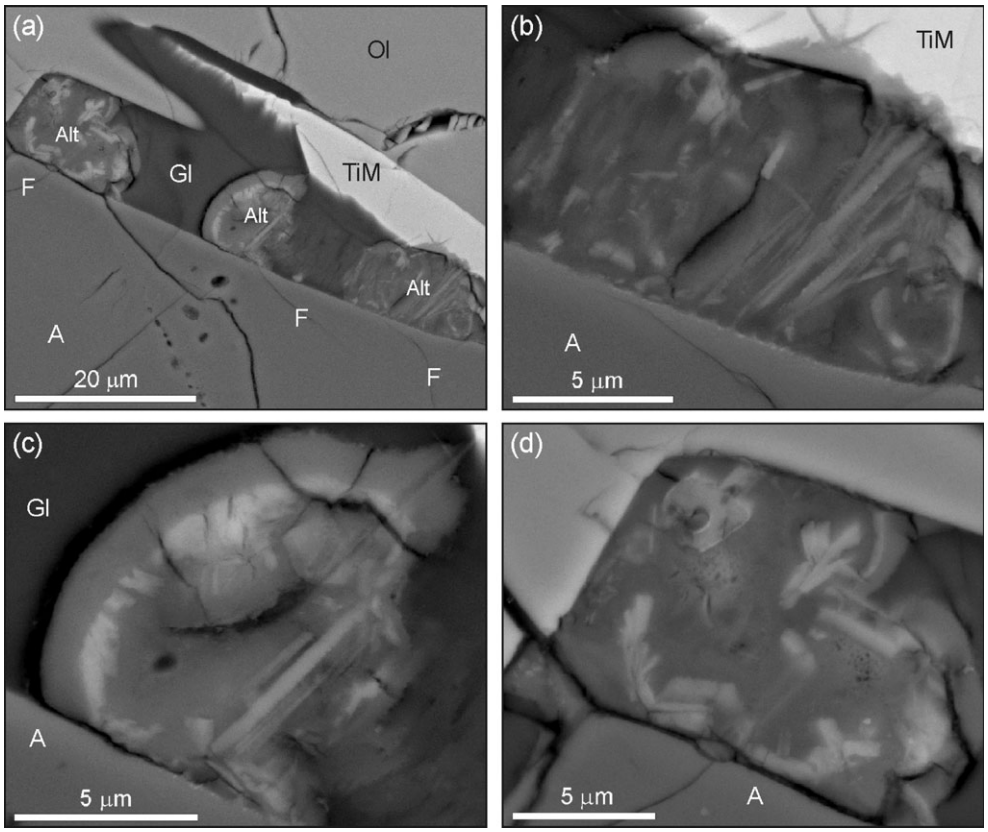

Fig. 1. BSE images of an olivine-hosted melt inclusion from BM1911. Glass (Gl) is surrounded by augite (A), titanomagnetite (TiM), and olivine (Ol). a) Three patches of glass-hosted alteration products (Alt). A hairline fracture (F) occurs within the augite beneath each patch. b–d) Images of the three patches, each of which comprises relatively high Z lath-shaped crystals within a much finer grained and lower Z groundmass. Foils for TEM work were extracted from the patches in (b) and (c).

growth of olivine crystals (Harvey and McSween 1992; Treiman 1993; Goodrich et al. 2013). Harvey and McSween (1992) recognized two varieties of melt inclusion, termed "vitrophyric" and "monocrystalline." The former are characterized by radiating sprays of acicular augite crystals, whereas monocrystalline inclusions are dominated by a single subrounded augite grain that may have a "meniscus" of silica-rich glass; finely crystalline daughter minerals can also be present within the glass. The BM1911 and BM1913 samples each contain one altered monocrystalline melt inclusion, and both inclusions have been studied here. Comparisons are also made with aqueously altered vitrophyric inclusions that were described from Nakhla by Goodrich et al. (2013).

Alteration Products within Olivine-Hosted Melt Inclusions

The BM1911 melt inclusion comprises two augite crystals, between which is a Na- and K-bearing aluminosilicate glass. One of the augite crystals is also partially enclosed by a glass meniscus (Fig. 1a). The BM1911 glass is similar in chemical composition to glasses that have been previously described from Nakhla melt inclusions (Table 1). The meniscus

Table 1. Chemical compositions of glass within Nakhla melt inclusions.

	BM1911	BM1913		H&McS (1992)[1]	Treiman (1993)	
SiO_2	63.98	68.44	68.38	70.03	74.84	64.41
TiO_2	0.15	d.l.	d.l.	0.09	0.21	0.14
Al_2O_3	19.83	18.57	18.91	14.84	16.19	17.00
Cr_2O_3	n.a.	d.l.	d.l.	n.a.	0.02	0.00
FeO	1.30	1.14	1.08	1.24	0.75	1.67
NiO	n.a.	n.a.	n.a.	n.a.	0.02	n.a.
MnO	0.17	d.l.	d.l.	0.05	0.01	0.00
MgO	0.23	0.16	d.l.	0.19	0.03	0.55
CaO	1.78	0.56	0.46	3.33	1.68	3.06
Na_2O	3.02	4.94	4.78	2.70	1.22	1.36
K_2O	5.52	7.27	7.18	5.08	4.85	5.11
P_2O_5	n.a.	n.a.	n.a.	n.a.	0.59	1.05
Total	95.98	101.08	100.79	97.54	100.40	94.34

[1]Analysis of Nakhla melt inclusion NK3 in Harvey and McSween (1992).
d.l. = below detection limits; n.a. = not analyzed.

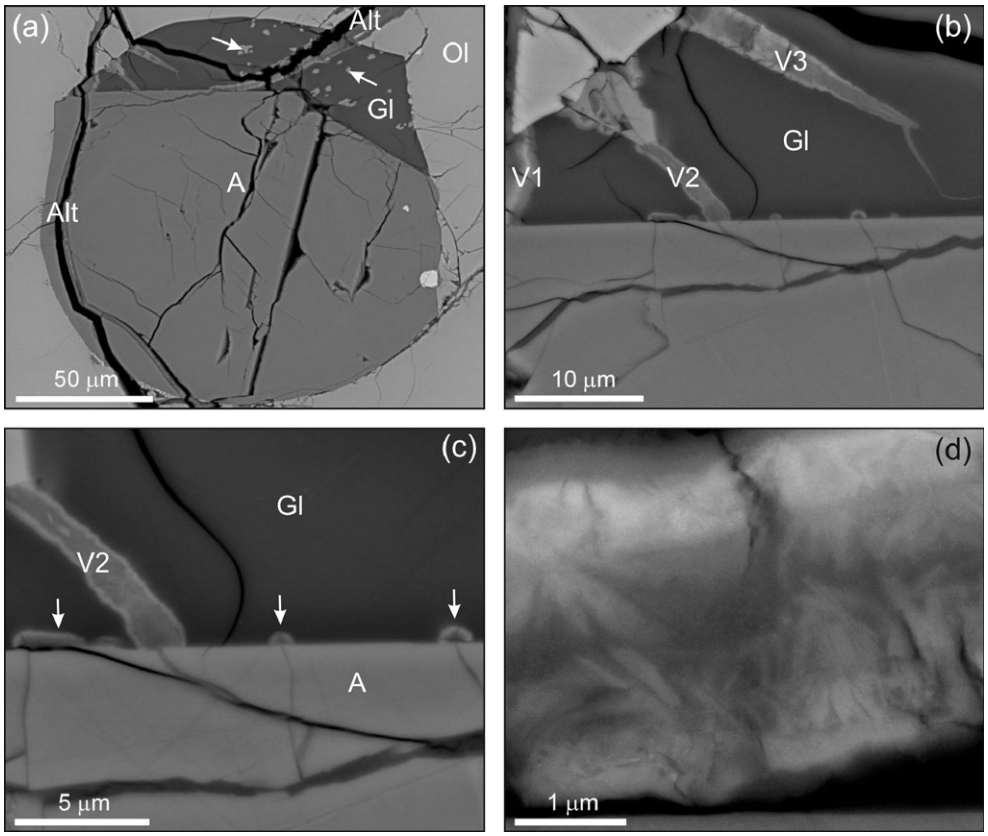

Fig. 2. BSE images of the BM1913 melt inclusion, which contains augite (A), glass (Gl), and alteration products. a) The whole melt inclusion. It comprises a crystal of augite and a meniscus of glass, and is enclosed by olivine (Ol). Veins of alteration products (Alt) occur in the augite, olivine, and glass. Glass also contains crystals of apatite (arrowed). b) The left-hand edge of the glass meniscus, which contains three alteration product veins, labeled V1, V2, V3. c) The interface between glass and augite that is decorated by three patches of alteration products (arrowed). Each patch is connected to a very narrow vein in the augite, as is vein V2. d) The interior of the largest of the glass-hosted veins (V4), which is seen in (a) toward the right-hand side of the meniscus. Its constituents comprise radiating arrays of laths in a lower Z groundmass.

contains three patches of alteration products, the largest of which is 10 μm in size (Figs. 1a–d). A hairline fracture is present within augite abutting each of the patches (Fig. 1a). BSE images show that the patches are composed of a very fine-grained and relatively low Z material that encloses higher-Z laths that are ~0.5 μm in thickness and a maximum of ~8 μm in length. These laths occur together as radiating sprays or as bundles of parallel crystals (Figs. 1b–d).

The BM1913 melt inclusion comprises a single crystal of augite. On one side of this crystal is a meniscus of Na- and K-bearing aluminosilicate glass (Fig. 2a), which is again similar in composition to other Nakhla glasses (Table 1). It contains 2–6 μm size euhedral crystals of apatite (Fig. 2a) together with four veins and four patches of alteration products (Figs. 2a–c). The patches are hemispherical or bulbous in shape, 1–3 μm in diameter, and decorate the contact between augite and glass (Figs. 2b and 2c). The veins contain relatively high Z laths that are comparable in size and shape to those in the BM1911 melt inclusion (Fig. 2d). All of the glass-hosted veins and patches are connected to veins in the surrounding augite and olivine grains (Figs. 2a–c).

SEM-EDX analyses of glass-hosted veins and patches are listed in Table 2, and plotted in Fig. 3. These alteration products are rich in Mg, Al, Si, and Fe, and their low analytical totals indicate the presence of water/OH. Veins within adjacent olivine grains have higher concentrations of Si and Mg, and lower concentrations of Al and Fe. The one augite-hosted vein that was sufficiently large to chemically analyze is depleted relative to alteration products within the glass with respect to Al and Fe, and is enriched in Mg and Ca (Table 2).

TEM images of foils that were extracted from two of the patches of alteration products in the BM1911 melt inclusion (Figs. 1b and 1c) show that they contain equant and lath-shaped crystals in a very fine-grained groundmass (Fig. 4a). The equant crystals are a few

Table 2. Chemical compositions of alteration products within Nakhla melt inclusions.

	BM1911	BM1913			
	Glass-hosted[1]	Glass-hosted[2]	Olivine-hosted[3]	Augite-hosted[4]	Goodrich et al.[5]
SiO_2	30.86	34.46	41.33	35.97	41.80
TiO_2	0.06	0.04	d.l.	d.l.	0.05
Al_2O_3	10.40	9.78	3.29	3.03	5.03
Cr_2O_3	n.a.	d.l.	d.l.	d.l.	n.a.
FeO	35.89	31.46	27.36	22.95	30.70
MnO	0.43	0.33	0.41	0.36	0.32
MgO	3.92	5.28	8.02	9.02	6.18
CaO	0.53	1.02	0.76	4.20	1.49
Na_2O	0.24	1.15	0.87	0.55	0.30
K_2O	0.65	1.30	1.05	0.62	1.08
P_2O_5	0.27	n.a.	n.a.	n.a.	0.57
F	n.a.	n.a.	n.a.	n.a.	0.15
Cl	n.a.	n.a.	n.a.	n.a.	0.45
Total	83.25	84.82	83.09	76.70	88.10

[1]Mean of five SEM-EDX analyses of patches.
[2]Mean of nine SEM-EDX analyses of veins.
[3]Mean of three SEM-EDX analyses of veins.
[4]Analysis of one vein by SEM-EDX.
[5]Mean of four analyses in Goodrich et al. (2013).
d.l. = denotes below detection limits; n.a. = denotes not analyzed.

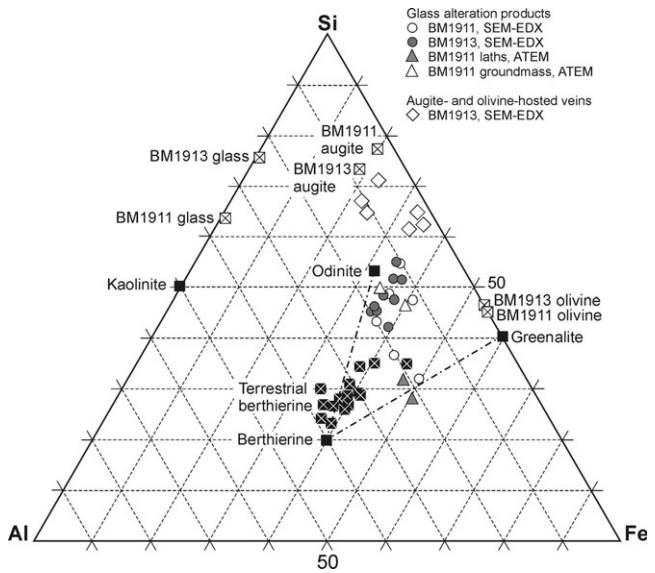

Fig. 3. Si-Al-Fe ternary diagram (atomic proportions). Components of the BM1911 and BM1913 melt inclusions are plotted using white and gray symbols. Also shown is stoichiometric berthierine, kaolinite, greenalite, and odinite (black squares). Analyses of terrestrial berthierine in Brindley (1982) are plotted using black squares with a white cross. ATEM analyses of the BM1911 laths plot along the line between stoichiometric berthierine and greenalite.

hundred nanometers in size. SAED patterns and ATEM data identify them as an aluminous clinopyroxene ($En_{38-48}Fs_{49-59}Wo_3$) (Table 3). The laths are ~1 μm length by ~0.3 μm in width. SAED patterns and lattice fringe images show that they have a ~0.7 nm basal layer spacing that is consistent with a serpentine group mineral (Fig. 4b). ATEM data from these laths reveal an Al-Fe silicate composition (Table 4). The two serpentine minerals that are rich in Al and Fe are berthierine, $Fe^{2+}{}_2Al_2SiO_5(OH)_4$, and odinite, $(Fe^{3+},Fe^{2+},Mg,Al,Ti,Mn)_{2.5}(Si,Al)_2O_5(OH)_4$. The best match for Nakhla lath chemistry is berthierine (Table 4, Fig. 3). This serpentine is compositionally very similar to iron-rich chlorite (Brindley 1982), but the two minerals can be distinguished by electron (and X-ray) diffraction by their basal layer spacings of 0.7 nm and 1.4 nm, respectively (Brindley 1982). The BM1911 laths have higher atomic Fe/Al and Fe/Si ratios than most of the analyses of terrestrial berthierine in Brindley (1982), and their Al/Si values are at the lower end of the range (Table 4, Fig. 3). This depletion of Al and enrichment of Fe relative to Si may reflect the substitution of Al^{3+} by Fe^{3+}. Alternatively, the chemical compositions of the laths may be due to the interstratification of layers of berthierine with greenalite, $(Fe^{2+},Fe^{3+})_3Si_2O_5(OH)_4$, and this possibility is supported by the fact that ATEM analyses plot on a line between the two serpentine minerals (Fig. 3).

The only constituents of the groundmass that could be identified by TEM imaging were fine fibers, some of which radiate from the laths and so appear to have used them as a substrate for growth (Figs. 4a and 4c). Individual crystals are too small for their d-spacings to be measured by SAED, but high-resolution imaging shows that they have ~0.7 nm lattice fringes, which is again consistent with serpentine (Fig. 4d). SAED patterns that were obtained from the groundmass as a whole contain diffuse rings, the three most intense of which have d-spacings of 0.437, 0.254, and 0.150 nm (Fig. 4a). These patterns indicate that the groundmass contains randomly oriented nanocrystals. ATEM analyses of the groundmass have lower Al/Si and Fe/Si values than the berthierine laths (Table 4, Fig. 3).

DISCUSSION

Evidence for Aqueous Alteration of Melt Inclusion Glass

The petrographic context of the veins and patches of alteration products within melt inclusions is consistent with their formation by water-mediated replacement of glass. This origin is revealed most clearly by the four patches in BM1913, each of which is located where an augite-hosted vein meets the glass meniscus (Fig. 2b). The presence of hairline fractures in augite immediately adjacent to the three alteration product patches in the BM1911 melt inclusion is likewise consistent with aqueous solutions having gained access

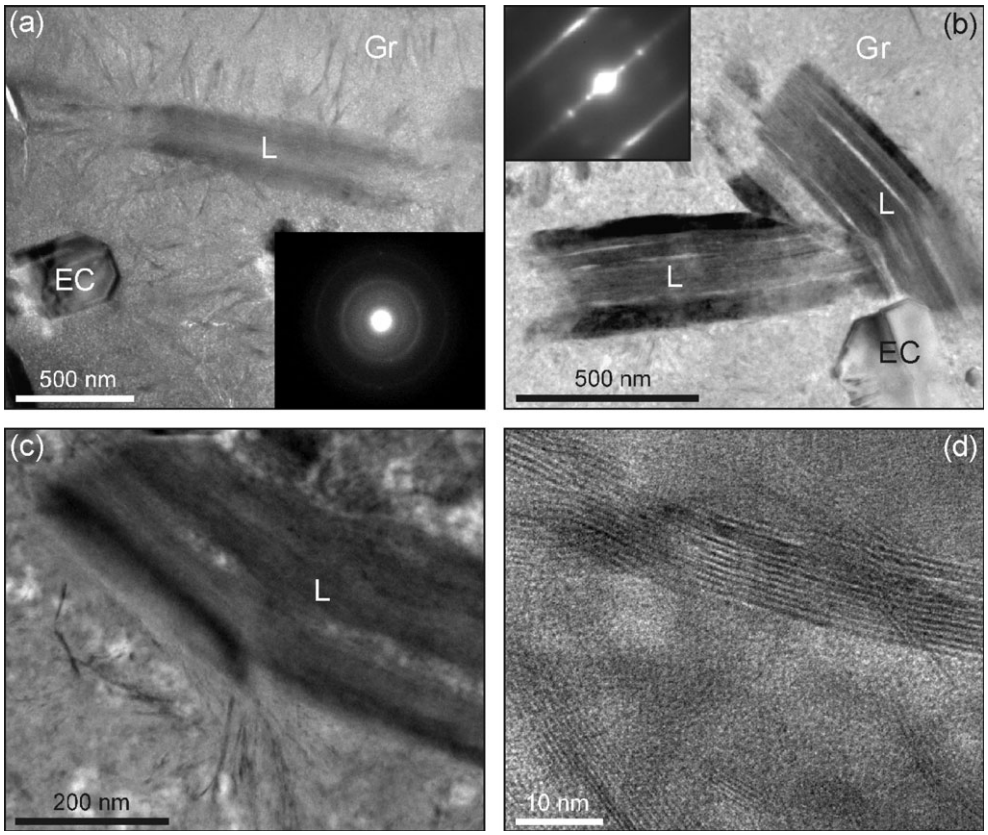

Fig. 4. TEM results from alteration products in the BM1911 melt inclusion. They have three constituents: equant crystals (EC), coarse laths (L), and a fine-grained groundmass (Gr). a) Bright-field image showing all of the constituents. Note that fibrous crystals in the groundmass radiate from a lath in the upper part of the image. A SAED pattern of the groundmass is inset. b) Bright-field image of two coarse laths, with an equant crystal in the lower right-hand corner. The inset SAED pattern is from the lath on the right-hand side, and its spots have a d-spacing of ~0.7 nm. c) Bright-field image of a lath and the groundmass. Fibrous crystals project into the groundmass from the lower edge of the lath. d) High-resolution image of the groundmass. Lattice fringes with a ~0.7 nm spacing highlight the presence of fine fibrous crystals in a variety of orientations.

to the glass via narrow channels in enclosing mineral grains. Equant crystals of clinopyroxene that occur in the BM1911 alteration products are interpreted to have originally been daughter crystals within the glass that were preserved intact during aqueous alteration (i.e., under the ambient physico-chemical conditions, clinopyroxene was less susceptible to replacement than glass). The bulbous and hemispherical shapes of alteration product patches suggest that they grew by radial expansion of a replacement front from the vein-glass contact. Similar microstructures characterize palagonite, which is a clay-rich product of the aqueous alteration of terrestrial volcanic glass (e.g., Stronick and Schmincke 2002). In contrast to the patches, veins that cross-cut BM1913 glass cannot have formed by a replacement front expanding radially outwards from a discrete point. These veins are more likely to have been produced by replacement of the walls of fractures within the glass that were continuous with fractures in augite and olivine grains.

Alteration products were described from within Nakhla polymineralic (vitrophyric) melt inclusions by Goodrich et al. (2013). Their chemical composition is quite similar to that of olivine-hosted veins in BM1913 (Table 2), and Goodrich et al. (2013) concluded that the alteration products had formed at the expense of feldspar, pyroxene, and glass. They also noted of the alteration products that they sometimes appear "to have been intruded into the inclusions from veins in the surrounding olivine" (Goodrich et al. 2013, p. 2378). Thus, we conclude that both the vitrophyric and monocrystalline melt inclusion were altered in a similar manner, namely by replacement mediated by liquid water that gained access to the glass via fractures in surrounding silicate mineral grains.

Conditions Promoting Berthierine Formation

The crystallographic and chemical properties of the laths that have formed by aqueous alteration of

Table 3. ATEM analyses of equant clinopyroxene crystals within glass alteration products.

	Equant crystal 1	Equant crystal 2
SiO_2	50.27	41.13
TiO_2	d.l.	d.l.
Al_2O_3	5.64	7.92
Cr_2O_3	d.l.	d.l.
FeO	27.13	35.47
MnO	0.81	1.08
MgO	14.95	12.78
CaO	1.17	1.61
Na_2O	d.l.	d.l.
Total	100.00	100.00
	Cations per 6 O	
Si	1.916	1.672
Ti	—	—
Al	0.253	0.379
Cr	—	—
Fe	0.865	1.206
Mn	0.026	0.037
Mg	0.849	0.774
Ca	0.048	0.070
Na	—	—
Total	3.958	4.138
Wo	2.7	3.4
En	48.2	37.8
Fs	49.1	58.8

d.l. = below detection limits; — = not applicable.

BM1911 glass are consistent with berthierine. Their depletion in Al and enrichment in Fe relative to the ideal composition of berthierine and terrestrial occurrences (Brindley 1982) are most likely due to interstratification with the Fe-serpentine mineral greenalite. Assuming that serpentine fibers in the groundmass are similar in chemical composition to the laths, ATEM results from the groundmass as a whole suggest that the fibers are contained within a material that is richer in Si than serpentine. The Si-rich material is proposed to be opaline silica given that opal-A is the main constituent of Nakhla olivine-hosted veins (Lee et al. 2015a). The inferred presence of opal-A is consistent with the composition of glass alteration products as determined by SEM-EDX. The interaction volume of these analyses will have encompassed both laths and groundmass, and accordingly in a Si-Al-Fe ternary diagram the alteration products plot between olivine-hosted veins (which contain opal-A) and berthierine (Fig. 3). Opal-A particles were not observed in the groundmass, but this is probably because this study did not use the appropriate imaging techniques (i.e., high-resolution scanning TEM imaging coupled with X-ray and electron spectroscopy; Lee et al. 2015a). Thus, we conclude that aqueous alteration of melt inclusion glass produced berthierine and opaline silica.

As the Nakhla melt inclusions contain a precursor phase (glass) and its replacement products (opal-A and berthierine), the mobility of cations during alteration can be tracked using the SEM-EDX data. Relative to Si, Mg and Fe were imported into the glass and Na and K were exported. By contrast, the mean Al/Si ratios (atomic) of glass and its alteration products are similar (BM1911 = 0.36 and 0.41, respectively; BM1913 = 0.32 and 0.34, respectively). Magnesium and Fe are interpreted to have been sourced from olivine, and Lee et al. (2013, 2015a) found good evidence in Nakhla for congruent dissolution of this mineral. The sink for alkali elements that were exported from the glass was probably the olivine-hosted veins, which contain an average of 0.87 wt% Na_2O and 1.05 wt% K_2O (Table 2). Lee et al. (2015a) suggested that alkali elements in the olivine-hosted veins had been sourced from the dissolution of mesostasis plagioclase feldspar, and so the present study demonstrates that Na and K were also derived from melt inclusion glass. The retention of Al in the glass alteration products suggests that the solutions were circumneutral (Al is least soluble at pH ~5–9; Hurowitz et al. 2006), and the import of Fe indicates reducing conditions. These conclusions are commensurate with the stability of berthierine in pE-pH space (i.e., pE~10 to −15 and pH ≥~7; Chevrier et al. 2007). The presence of opal-A in the groundmass is also consistent with circumneutral solutions since the solubility of silica is very low below pH8 (Alexander et al. 1954). As berthierine transforms to chlorite at temperatures in excess of ~70 °C (Hornibrook and Longstaffe 1996), Nakhla must have remained at a relatively low temperature following serpentinization, and this conclusion is consistent with the preservation of opal-A. It is unlikely that berthierine laths and the opal-A formed simultaneously, but their relative timing of precipitation is difficult to determine from the petrographic evidence alone.

The Environment of Water/Rock Interaction

Berthierine is a new addition to the suite of secondary hydrous silicates that have been described from Nakhla (Table 5), most of which occur in the olivine-hosted veins. Chatzitheodoridis et al. (2014) documented iron-rich saponite that had formed as a rind around a vesicle in mesostasis glass, and so the petrographic context of this mineral is similar to that of berthierine.

Two styles of water/rock interaction could account for the diversity of secondary silicates in Nakhla (1) the introduction of multiple generations of solutions of

Table 4. Chemical compositions of the products of aqueous alteration of Nakhla melt inclusions compared with terrestrial berthierine.

	Lath[1]	Lath[1]	Berthierine[2]	Groundmass[1]	Groundmass[1]
SiO_2	24.52	27.20	22.03	42.06	38.76
TiO_2	d.l.	d.l.	3.63	d.l.	d.l.
Al_2O_3	16.49	15.47	22.91	12.28	9.82
Cr_2O_3	d.l.	d.l.	0.05	d.l.	d.l.
Fe_2O_3	n.a.	n.a.	0.46	d.l.	d.l.
FeO	53.27	50.09	36.68	34.53	41.74
MnO	0.75	0.70	0.04	0.63	0.67
MgO	2.35	3.67	1.91	7.95	6.46
CaO	0.31	0.11	0.07	0.17	0.06
Na_2O	1.40	1.92	0.08	1.05	1.18
K_2O	0.92	0.85	0.03	1.33	1.32
H_2O	n.a.	n.a.	11.28	d.l.	d.l.
Total	100.01	100.01	100.05	100.00	100.00
		On the basis of 28 O			
Si^{4+}	5.316	5.760	4.972		
$^{IV}Al^{3+}$	2.684	2.240	3.028		
$^{VI}Al^{3+}$	1.529	1.620	3.064		
Ti^{4+}	—	—	0.616		
Cr^{3+}	—	—	0.009		
Fe^{2+}	9.658	8.871	7.000		
Mn^{2+}	0.138	0.126	0.008		
Mg^{2+}	0.759	1.159	0.643		
Ca^{2+}	0.072	0.025	0.017		
Na^{+}	0.588	0.788	—		
K^{+}	0.254	0.230	0.009		
Total	20.999	20.818	19.36		
Total tet.	8.000	8.000	8.000		
Total oct.	12.999	12.818	11.365		

[1]TEM-EDX data, normalized to 100 wt%.
[2]Mean of 14 analyses of terrestrial berthierine in Brindley (1982). The data are also plotted in Fig. 3.
d.l. = below detection limits; n.a. = not analyzed; — = not applicable.

Table 5. Hydrous silicate alteration products previously described from Nakhla.

Hydrous silicate	References
Colloidal material/ amorphous gel	Ashworth and Hutchison (1975), Changela and Bridges (2011)
Opal-A	Lee et al. (2015a)
Serpentine	Treiman and Gooding (1991), the present study
Smectite (including saponite)	Wentworth and Gooding (1990), Gooding et al. (1991), Treiman and Gooding (1991), Bridges and Grady (2000), Lee et al. (2013), Chatzitheodoridis et al. (2014)

differing chemical composition, possibly over an extended period of time, or (2) the presence of chemically distinct microenvironments reflecting local (i.e., sub-millimeter length scale) variations of solution compositions in a system with low water/rock ratios. Results presented here are more consistent with the second scenario, although solution chemistry could also have varied over time at any one site, as was proposed by Chatzitheodoridis et al. (2014) to account for growth of a multilayered saponite ovoid. The clearest petrographic evidence for spatial partitioning of fluid compositions (i.e., chemical microenvironments) is that berthierine occurs only in the parts of veins that cross-cut melt inclusion glass (i.e., berthierine is absent from augite- and olivine-hosted veins). Indeed there has been only one, tentative, description of serpentine from olivine-hosted veins in Nakhla despite the considerable amount of TEM work that been undertaken on them (e.g., Ashworth and Hutchison 1975; Gooding et al. 1991; Treiman and Gooding 1991; Changela and Bridges 2011; Lee et al. 2013, 2015a) (Table 5). The control on the chemical composition and mineralogy of alteration products (i.e., berthierine) by their host phase (i.e., glass) is consistent with their formation by interface-coupled dissolution-precipitation, as described

above. A close correspondence between the chemical composition of alteration products and their host phase has also been described from the Lafayette meteorite (Treiman 1993; Hicks et al. 2014; Lee et al. 2015b), thus indicating that physico-chemical conditions were similar within the nakhlite parent rock(s).

In addition to hydrous silicates, Nakhla contains carbonates (Carr et al. 1985; Chatzitheodoridis and Turner 1990), Fe-oxyhydroxides (Treiman and Gooding 1991), gypsum, and halite (Chatzitheodoridis and Turner 1990; Gooding et al. 1991). Petrographic evidence shows that the carbonates are formed following the introduction of CO_2-charged groundwaters and by replacement of olivine-hosted veins (Lee et al. 2015a). A proportion of the Fe-oxyhydroxides were produced by oxidation of carbonate, which could have taken place before or after Nakhla fell to Earth (Lee et al. 2015a). Gypsum and halite indicate the presence of saline solutions, although it is possible that the sulfates could have formed by terrestrial weathering before and/or during museum curation (Gooding et al. 1991).

Other Descriptions of Serpentine and Al-Rich Phyllosilicates in the Martian Crust

Serpentine occurs in several nakhlite meteorites in addition to Nakhla. This phyllosilicate was proposed as a possible constituent of olivine-hosted veins from Miller Range 03346 (Imae and Ikeda 2007), and the presence of serpentine was confirmed by Noguchi et al. (2009) in a TEM study of Yamato 000593 and 000749. Changela and Bridges (2011) and Hicks et al. (2014) subsequently described serpentine from the mesostasis of Lafayette; Changela and Bridges (2011) suggested that it may be berthierine, whereas the later study concluded that this mineral was a Fe-serpentine.

The Al-rich phyllosilicates chlorite, kaolinite, and montomorillonite have been described from a few localities on Mars using orbital remote sensing (Mustard et al. 2008; Wray et al. 2008). Those minerals found by Wray et al. (2008) occur in discrete layers within the stratigraphy of Mawrth Vallis, and the Al-rich clays are interpreted to have formed by alteration of volcanic glass within pyroclastic deposits. Ehlmann et al. (2010) sought chamosite and berthierine using data from CRISM on the Mars Reconnaissance Orbiter but were unable to detect either mineral. They did, however, find that Mg-serpentine occurs in several Noachian terranes of southern highlands where it is inferred to have formed by the hydrothermal alteration of ultramafic rocks. Results of this study confirm that water-mediated alteration of igneous glass can produce Al-rich phyllosilicates, although the berthierine occurs in Nakhla in such small quantities as to be undetectable by orbital spectroscopy.

CONCLUSIONS

1. Interaction of atmospherically derived water with the part of the igneous crust of Mars that was sampled by Nakhla has formed the hydrous silicates saponite, opal-A and berthierine;
2. This diversity of silicate alteration products reflects low water/rock ratios. These conditions created microenvironments whose chemistry was largely determined by the compositions of those primary components that were reacting most rapidly with liquid water (i.e., olivine and glass);
3. Berthierine formed by the replacement of aluminosilicate glass in olivine-hosted melt inclusions;
4. By analogy with Nakhla, the scarcity of Al-rich phyllosilicates in the Martian crust more broadly reflects low water/rock ratios and the circumneutral pH of the solutions, which together have militated against aqueous transport and concentration of Al and Si.

Acknowledgments—We thank Billy Smith, Colin How, and Sam MacFadzean for help with the FIB and TEM; Peter Chung for assistance with the SEM; and the Natural History Museum (London) for loan of the Nakhla samples. The authors are grateful to Allan Treiman and an anonymous reviewer for comments that have significantly improved this manuscript. This work was funded by the UK STFC through grants ST/H002960/1, ST/K000942/1, and ST/L002167/1, and supported by COST Action TD 1308.

Editorial Handling—Dr. Ed Scott

REFERENCES

Alexander G. B., Heston W. M., and Iler R. K. 1954. The solubility of amorphous silica in water. *The Journal of Physical Chemistry* 58:453–455.

Ashworth J. R. and Hutchison R. 1975. Water in non-carbonaceous stony meteorites. *Nature* 256:714–715.

Boctor N.Z., Alexander C. M. O'D., Wang J., and Hauri E. 2003. The sources of water in Martian meteorites: Clues from hydrogen isotopes. *Geochimica et Cosmochimica Acta* 67:3971–3989.

Bridges J. C. and Grady M. M. 2000. Evaporite mineral assemblages in the nakhlite (Martian) meteorites. *Earth and Planetary Science Letters* 176:267–279.

Brindley G. W. 1982. Chemical compositions of berthierines—A review. *Clays and Clay Minerals* 30:153–155.

Bunch T. E. and Reid A. M. 1975. The nakhlites Part 1: Petrography and mineral chemistry. *Meteoritics* 10:303–315.

Carr R. H., Grady M. M., Wright I. P., and Pillinger C. T. 1985. Martian atmospheric carbon dioxide and weathering products in Mars meteorites. *Nature* 314:248–250.

Changela H. G. and Bridges J. C. 2011. Alteration assemblages in the nakhlites: Variation with depth on Mars. *Meteoritics & Planetary Science* 45:1847–1867.

Chatzitheodoridis E. and Turner G. 1990. Secondary minerals in the Nakhla meteorite. *Meteoritics* 25:354.

Chatzitheodoridis E., Haigh S., and Lyon I. 2014. A conspicuous clay ovoid in Nakhla: Evidence for subsurface hydrothermal alteration on Mars with implications for astrobiology. *Astrobiology* 14:651–693.

Chevrier V., Poulet F., and Bibring J.-P. 2007. Early geochemical environment of Mars as determined from thermodynamics of phyllosilicates. *Nature* 448:60–63.

Ehlmann B. L., Mustard J. F., and Murchie S. L. 2010. Geological setting of serpentine deposits on Mars. *Geophysical Research Letters* 37:L06201.

Friedman-Lentz R. C., Taylor G. J., and Treiman A. H. 1999. Formation of a martian pyroxenite: A comparative study of the nakhlite meteorites and Theo's Flow. *Meteoritics & Planetary Science* 34:919–932.

Gooding J. L., Wentworth S. J., and Zolensky M. E. 1991. Aqueous alteration of the Nakhla meteorite. *Meteoritics* 26:135–143.

Goodrich C. A., Treiman A. H., Filiberto J., Gross J., and Jercinovic M. 2013. K_2O-rich trapped melt in olivine in the Nakhla meteorite: Implications for petrogenesis of nakhlites and evolution of the Martian mantle. *Meteoritics & Planetary Science* 48:2371–2405.

Hallis L. J., Taylor G. J., Nagashima K., Huss G. R., Needham A. W., Grady M. M., and Franchi I. A. 2012a. Hydrogen isotope analyses of alteration phases in the nakhlite Martian meteorites. *Geochimica et Cosmochimica Acta* 97:105–119.

Hallis L. J., Taylor G. J., Nagashima K., and Huss G. R. 2012b. Magmatic water in the martian meteorite Nakhla. *Earth and Planetary Science Letters* 359–360:84–92.

Harvey R. P. and McSween H. Y. 1992. The parent magma of the nakhlite meteorites: Clues from melt inclusions. *Earth and Planetary Science Letters* 111:467–482.

Hicks L. J., Bridges J. C., and Gurman S. J. 2014. Ferric saponite and serpentine in the nakhlitemartian meteorites. *Geochimica et Cosmochimica Acta* 136:194–210.

Hornibrook E. R. C. and Longstaffe F. J. 1996. Berthierine from the lower Cretaceous Clearwater formation, Alberta, Canada. *Clays and Clay Minerals* 44:1–21.

Hu S., Lin Y., Zhang J., Hao J., Feng L., Xu L., Yang W., and Yang J. 2014. NanoSIMS analyses of apatite and melt inclusions in the GRV 020090 Martian meteorite: Hydrogen isotope evidence for recent past underground hydrothermal activity on Mars. *Geochimica et Cosmochimica Acta* 140:321–333.

Hurowitz J. A., McLennan S. M., Tosca N. J., Arvidson R. E., Michalski J. R., Ming D. W., Schroder C., and Squyres S. W. 2006. In situ and experimental evidence for acidic weathering of rocks and soils on Mars. *Journal of Geophysical Research-Planets* 111:E02S19.

Imae N. and Ikeda Y. 2007. Petrology of the Miller Range 03346 nakhlite in comparison with the Yamato-00593 nakhlite. *Meteoritics & Planetary Science* 42:171–184.

Karlsson H. R., Clayton R. N., Gibson E. K. Jr, and Mayeda T. K. 1992. Water in SNC meteorites: Evidence for a Martian hydrosphere. *Science* 255:1409–1411.

Lee M. R., Bland P. A., and Graham G. 2003. Preparation of TEM samples by focused ion beam (FIB) techniques: Applications to the study of clays and phyllosilicates in meteorites. *Mineralogical Magazine* 67:581–592.

Lee M. R., Tomkinson T., Mark D. F., Stuart F. M., and Smith C. L. 2013. Evidence for silicate dissolution on Mars from the Nakhla meteorite. *Meteoritics & Planetary Science* 48:224–240.

Lee M. R., MacLaren I., Andersson S. M. L., Kovacs A., Tomkinson T., Mark D. F., and Smith C. L. 2015a. Opal-A in the Nakhla meteorite: A tracer of ephemeral liquid water in the Amazonian crust of Mars. *Meteoritics & Planetary Science* 50:1362–1377.

Lee M. R., Tomkinson T., Hallis L. J., and Mark D. F. 2015b. Formation of iddingsite veins in the Martian crust by centripetal replacement of olivine: Evidence from the nakhlite meteorite Lafayette. *Geochimica et Cosmochimica Acta* 154:49–65.

Leshin L. A., Epstein S., and Stolper E. M. 1996. Hydrogen isotope geochemistry of SNC meteorites. *Geochimica et Cosmochimica Acta* 60:2635–2650.

McSween H. Y. Jr. 1985. SNC Meteorites: Clues to Martian petrologic evolution? *Reviews in Geophysics* 23:391–416.

McSween H. Y. Jr. 1994. What we have learned about Mars from SNC meteorites. *Meteoritics* 29:757–779.

Mustard J. F., Murchie S. L., Pelkey S. M., Ehlmann B. L., Milliken R. E., Grant J. A., Bibring J.-P., Poulet F., Bishop J., Dobrea E. N., Roach L., Seelos F., Arvidson R. E., Wiseman S., Green R., Hash C., Humm D., Malaret E., McGovern J. A., Seelos K., Clancy T., Clark R., Marais D. D., Izenberg N., Knudson A., Langevin Y., Martin T., McGuire P., Morris R., Robinson M., Roush T., Smith M., Swayze G., Taylor H., Titus T., and Wolff M. 2008. Hydrated silicate minerals on mars observed by the Mars reconnaissance orbiter CRISM instrument. *Nature* 454:305–309.

Needham A. W., Abel R. L., Tomkinson T., and Grady M. M. 2013. Martian subsurface fluid pathways and 3D mineralogy of the Nakhla meteorite. *Geochimica et Cosmochimica Acta* 116:96–110.

Noguchi T., Nakamura T., Misawa K., Imae N., Aoki T., and Toh S. 2009. Laihunite and jarosite in the Yamato 00 nakhlites: Alteration products on Mars? *Journal of Geophysical Research* 114:E10004.

Prior G. T. 1912. The meteoric stones of El Nakhla El Baharia. *Mineralogical Magazine* 16:274–281.

Stronick N. A. and Schmincke H.-U. 2002. Palagonite — A review. *International Journal of Earth Science* 91:680–697.

Swindle T. D. and Olson E. K. 2004. Ar-40-Ar-39 studies of whole rock nakhlites: Evidence for the timing of formation and aqueous alteration on Mars. *Meteoritics & Planetary Science* 39:755–766.

Tomkinson T., Lee M. R., Mark D. F., and Smith C. L. 2013. Sequestration of Martian CO_2 by mineral carbonation. *Nature Communications* 4:2662.

Treiman A. H. 1993. The parent magma of the Nakhla (SNC) meteorite, inferred from magmatic inclusions. *Geochimica et Cosmochimica Acta* 57:4753–4767.

Treiman A. H. 2005. The nakhlite meteorites: Augite-rich igneous rocks from Mars. *Chemie der Erde* 65:203–270.

Treiman A. H. and Gooding J. L. 1991. Iddingside in the Nakhla meteorite: TEM study of mineralogy and texture

of pre-terrestrial (Martian?) alterations. *Meteoritics* 26:402.

Usui T., Alexander C. M. O'D., Wang J. H., Simon J. I., and Jones J. H. 2012. Origin of water and mantle-crust interactions on Mars inferred from hydrogen isotopes and volatile element abundances of olivine-hosted melt inclusions of primitive shergottites. *Earth and Planetary Science Letters 357–358* 11:9–129.

Usui T., Alexander C. M. O'D., Wang J. H., Simon J. I., and Jones J. H. 2015. Meteoritic evidence for a previously unrecognized hydrogen reservoir on Mars. *Earth and Planetary Science Letters* 410:140–151.

Velbel M. A. 2012. Aqueous alteration in Martian meteorites: Comparing mineral relations in igneous rockweathering of Martian meteorites and in the sedimentary cycle of Mars. In Sedimentary geology of Mars, edited by Grotzinger J. and Milliken R. *Society for Sedimentary Geology Special Publication* 102:97–117.

Velbel M. A. 2016. Aqueous corrosion of olivine in the Mars meteorite Miller Range (MIL) 03346 during Antarctic weathering: Implications for water on Mars. *Geochimica et Cosmochimica Acta* 180:126–145.

Watson L. L., Hutcheon I. D., Epstein S., and Stolper E. M. 1994. Water on Mars: Clues from D/H and water contents of hydrous phases in SNC meteorites. *Science* 265:85–90.

Wentworth S. J. and Gooding J. L. 1990. Pre-terrestrial origin of "rust" in the Nakhla meteorite (abstract #1672). 21st Lunar and Planetary Science Conference. CD-ROM

Wray J. J., Ehlmann B. L., Squyres S. W., Mustard J. F., and Kirk R. L. 2008. Compositional stratigraphy of clay-bearing layered deposits at Mawrth Vallis, Mars. *Geophysical Research Letters* 35:L12202.